Ferromagnetism in ferroelectric BaTiO_{3} induced by vacancies: Sensitive dependence on charge state, origin of magnetism, and temperature range of existence

Aldo Raeliarijaona and Huaxiang Fu

Ferromagnetism in ferroelectric BaTiO$_3$ induced by vacancies: sensitive dependence on charge state, origin of magnetism, and temperature range of existence

Aldo Raeliarijaona[1,2] and Huaxiang Fu[1]

[1]*Department of Physics, University of Arkansas, Fayetteville, Arkansas 72701, USA*
[2]*Department of Physics, Applied Physics, and Astronomy,*
Rensselaer Polytechnic Institute, Troy, New York 12180, USA
(Dated: July 21, 2017)

Using density-functional calculations we investigate the possibility and underlying mechanism of generating ferromagnetism (FM) in ferroelectric (FE) BaTiO$_3$ by native vacancies. For the same vacancy species but different charge states (e.g., V_O^0 vs V_O^{2+}), our study reveals a marked difference in magnetic behaviors. For instance, while V_O^0 is ferromagnetic, V_O^{2+} is not. This sensitive dependence, which was often overlooked, highlights the critical importance of taking into account different charge states. Furthermore, while oxygen vacancies have been often used in experiments to explain the vacancy-induced FM, our calculation demonstrates that Ti vacancies, in particular V_{Ti}^{3-} and V_{Ti}^{2-} with low formation energies, generate even stronger ferromagnetism in BaTiO$_3$, with a magnetic moment which is 400% larger than that of V_O^0. Interestingly, this strong FM of V_{Ti} can be further enhanced by hole doping. Although both cation vacancies (V_{Ti}^q) and anion vacancies (V_O^0) induce FM, their mechanisms differ drastically. FM of anion vacancies originates from the spin-polarized *electrons* at Ti sites, but FM of cation vacancies stems from the spin-polarized *holes* at O sites. This work also sheds new light on vacancy-induced FM by discovering that the spin densities of all three considered vacancy species are highly extended in real space, distributed far away from the vacancy. Moreover, we predict that the ferromagnetism caused by V_{Ti}^{3-} is able to survive at high temperatures, which is promising for room-temperature spintronic or multiferroic applications.

PACS numbers: 77.84.-s, 61.72.jd

I. INTRODUCTION

Native vacancies in ferroelectric perovskites of switchable spontaneous polarization are of fundamental and technological relevance.[1,2] Fundamentally, the existence of vacancies breaks the delicate balance between long-range and short-range interactions in FEs,[3,4] thus profoundly affecting ferroelectricity. This may hamper the superior properties that have been found in FEs, such as high electromechanical response,[5–7] large dielectric coefficient,[8,9] enhanced polarization in superlattices,[10] composition-induced ferroelectricity,[11] strong trilinear coupling between rotation and polarization in improper ferroelectrics,[12–16] anti-ferroelectricity,[17,18] and unusual phase transitions[19–21]. Furthermore, vacancies also influence conductivity,[22] optical absorption,[23] and photorefractive index[24], showing widespread effects that span across different fields from material science to nonlinear optics. Technologically it is known that vacancies play a critical role in polarization switching by reducing ferroelectricity and by pinning polarization, which is one of the major causes for fatigue.[25–28] Vacancies also affect the stability of domain walls.[29–31] Interestingly, apart from the detrimental effects, vacancies may nevertheless bring favorable material properties, for example, Pb vacancies can broaden the dielectric peaks in disordered Pb(ScNb)O$_3$,[32] and furthermore, vacancies can enhance the piezoelectric response in aged BaTiO$_3$.[33] Also, vacancies were shown to increase significantly the local polarization in PbTiO$_3$ (Ref.34). The strong interest in studying vacancies stems from the fundamental importance of understanding new effects of these vacancies, and from the technological demand of achieving a better control of vacancies, either to suppress their detrimental effects and/or to enhance their desirable properties.

Recently, a new area of fundamental interest on vacancies emerges, that is, to understand the possibility and underlying physics of generating ferromagnetism by native vacancies in ferroelectrics. It is widely accepted that FE and FM are mutually incompatible in prototypical perovskite ferroelectrics of *perfect* crystal form, since the d orbitals of B-site atoms are empty, which does not favor FM.[35] However, once vacancies are created, this empty d-orbital rule no longer applies. Since FEs often possess strong spontaneous polarization, and under the assumption that vacancies are able to cause FM, there is possibility that multiferroic properties[36–39] could coexist in FEs with vacancies. Furthermore, because many FEs have a high Curie temperature in terms of ferroelectric phase transition, one may hope to find a way of creating room-temperature multiferroics. Indeed, there was experimental evidence showing FM hysteresis in BaTiO$_3$, when vacancies appear in samples by annealing at different oxygen pressures.[40] It was also reported experimentally that FM may exist at the *surface* of non-stoichiometric FE thin-films, while ferroelectricity persists in the *interior* of the films.[41]

Despite the importance of vacancy-induced FM in FEs, there is nevertheless insufficient understanding and sometimes even misconception in the literature regarding the subject. First, it is often assumed in experiments that oxygen vacancies (V_O) are the origin of FM.[40–43] What if samples are synthesized under the oxygen-rich condi-

tion in which V_O is unlikely to form? Will FM exist in BaTiO$_3$? How large will be the magnetic moment? Nowadays, with the contemporary advance in molecular beam epitaxy (MBE),[44] there is sophisticated control of FE fabrication, which allows a tuning of the growth condition so that a particular species of vacancies (e.g., either Ba or Ti vacancies) could appear. This provides possibility of controlling the magnetism in FEs by selectively choosing the vacancy species.

Second, the critical knowledge on how different charge states of a given vacancy species (e.g., V_{Ti}^{4-} versus V_{Ti}^{3-}) influence the magnetism in BaTiO$_3$—is not understood. Here we use the notation V_X^q to denote a vacancy of species X carrying a charge amount q. For instance, V_{Ba}^{1-} stands for a Ba vacancy carrying a negative charge $q = 1-$. By changing the chemical potential of electron reservoir (i.e., the Fermi energy of the system) during growth, it is known that different charge states of the same vacancy species could have very different vacancy formation energies and defect properties.[45,46] Indeed, charged defects were commonly detected in experiments by electron paramagnetic resonance (EPR).[47,48] However, some existing theoretical studies on vacancy-induced magnetism considered only the neutral vacancies.[49] While it is computationally convenient to investigate neutral vacancies, charged vacancies are more important and more likely to occur in solids. Take oxygen vacancy as an example. First-principles calculations have shown that charged vacancies V_O^{2+} and V_O^{1+} are energetically more stable than neutral V_O^0, for a wide range of the chemical potential of the electron reservoir.[50,51] Since V_O^{2+} and V_O^{1+} are more stable, we must consider these charge states and examine whether they will give rise to FM.

Furthermore, there is an often adopted, but unproven, rule related to this topic, namely that scientists often assume that an unpaired electron, e.g., in systems with an odd number of electrons in one unit cell, should have magnetism, since the odd number of electrons tends to create an unbalanced occupation between spin-up and spin-down states. According to this rule, oxygen vacancy V_O^{1+} with a charge state of $q = 1+$ has an unpaired electron and is expected to be magnetic. However, as will be shown below, this turns out to be incorrect.

Third, there is little understanding on what temperature range the vacancy-induced ferromagnetism may survive. The temperature range of FM existence is particularly relevant, since currently there is strong interest in pursuing FM, FE, and multiferroic that can work at room temperature. Furthermore, since different vacancy species introduce different interactions, it will be interesting to investigate how the temperature range of FM may differ (or resemble) for different vacancy species.

Finally, another important issue concerns how the induced magnetic spin density is distributed in the neighborhood of vacancy. Is the spin density very localized or rather extended? As pointed out by Moryia, there are two different descriptions of ferromagnetism: the local moment theory and the itinerant electron theory.[52] In the former, magnetism is caused by magnetic moments of localized electrons, where electrons are tightly bound to the nearest atoms, and the exchange interaction between electrons, with the help of Pauli's exclusion principle, causes the magnetic moments at different atoms to align or anti-align, forming an order-disorder type of phase transition. The exchange interaction may include direct exchange, superexchange, RKKY, and Zener double exchange.[53] In the itinerant electron theory, magnetism is initiated by the spin polarization of *delocalized* electrons, due to itinerant exchange. Although the spin polarization forces some electrons to occupy higher single-particle Kohn-Sham orbitals (thus costing energy), it nevertheless can reduce the Coulomb repulsive interaction among electrons of different spins (thus gaining energy). When the energy gain is larger than the energy cost (i.e., the Stoner criterion[54]), magnetization occurs. For vacancy-induced magnetism, it is not clear whether the magnetic moment is localized near the vacancy, or is spread over a considerable space region.

Considering the importance of the vacancy-induced FM, and furthermore, considering that there are critical issues that are unsettled, more studies are obviously needed to obtain better physics and understanding. The purpose of this paper is three-fold: (i) to determine what charge states of different vacancy species can induce FM in bulk BaTiO$_3$; (ii) to reveal the origin of the vacancy-induced FM and the nature of the spin-polarized magnetic moments; (iii) to find the temperature range within which the induced FM can sustain.

We show in this study that the charge state of vacancy is critical in terms of determining whether FM exists or not. For instance, while V_O^0 is FM, V_O^{1+} is not. The result highlights that we must consider specifically the charge state in order to obtain correct understanding of vacancy-induced FM. Our calculation also demonstrates that the rule of judging magnetism by counting the number of electrons is unjustified when it comes to the vacancy-induced FM in FEs. Furthermore, we reveal the origin of vacancy-induced FM in BaTiO$_3$, showing that the spin density is markedly spread in BaTiO$_3$, and vacancy-induced FM in this solid is better described by itinerant theory. Magnetism of V_O^0 is caused by the spin-polarization of itinerant electrons at Ti $3d$ orbitals, and in contrast, magnetism of V_{Ti}^{3-} originates from the the itinerant holes at O $2p$ orbitals. Moreover, the temperature range which magnetic moment can sustain is predicted to be drastically different for different vacancies. FM induced by V_{Ti}^{3-} is shown to be able to survive at room temperature, which is promising for potential spintronic or multiferroic applications.

It may be worth pointing out that, although studies on magnetism in another material PbTiO$_3$ exist,[55–57] the results of PbTiO$_3$, however, cannot be directly applied to BaTiO$_3$, due to rather drastic differences between two materials. In PbTiO$_3$, there are strong Pb-O hybridization, large c/a ratio, dissimilar Ti-O bonds (all of which do not exist in BaTiO$_3$). The strong Pb-O hybridiza-

tion in $PbTiO_3$ reveals that the interaction between A-site atoms and O atoms are different in $PbTiO_3$ and in $BaTiO_3$. Meanwhile, the large c/a ratio in $PbTiO_3$ indicates that the Ti-O interaction is also substantially different in two solids. These profound differences make the vacancy properties in these two solids very different. Furthermore, currently there is a strong interest in Pb-free ferroelectrics. $BaTiO_3$ is an important Pb-free material with strong ferroelectricity. The ferromagnetism in $BaTiO_3$ is thus more important than in $PbTO_3$.

Indeed we find many new results (including the origin of magnetism), regarding the ferromagnetism (FM) in $BaTiO_3$ as compared to $PbTiO_3$. More specifically, we find that (i) the charge states that possess FM could be very different in $BaTiO_3$ and in $PbTiO_3$. For instance, V_{O1}^0 is found in this study to be ferromagnetic in $BaTiO_3$, but V_{O1}^0 was reported[56] to be non-magnetic (NM) in $PbTiO_3$. Further, V_{Ba}^0 is FM in $BaTiO_3$, but V_{Pb}^0 is[56] NM in $PbTiO_3$, etc. These dissimilar behaviors manifest the differences in atomic interaction and chemical bonding of two materials. (ii) Our study shows that the spin density of magnetization $\Delta\rho(\mathbf{r}) = \rho_\uparrow(\mathbf{r}) - \rho_\downarrow(\mathbf{r})$ is highly *delocalized* and spreads over the entire solid in $BaTiO_3$, revealing that the origin of magnetism is itinerant. However, and in contrast, $\Delta\rho(\mathbf{r})$ in $PbTiO_3$ was shown[55] to be very *localized*, and is nonzero only in the nearest neighbor of the vacancy, showing that magnetism in $PbTiO_3$ originates from localized moments. (iii) The temperature dependence of magnetism is one key subject in our study, and we find that FM of V_{Ti}^{3-} can survive above room temperature. The subject has not been addressed previously in $PbTiO_3$.[55–57]

The paper is organized as follows. In Sec. II we describe the details of the computational methods. We then present in Sec. III the calculation results and relevant discussions. In Sec. IV, a summary is given to conclude the paper. In Appendix, the vacancy formation energy is calculated and the relevant growth condition for a chosen vacancy to occur in $BaTiO_3$ is discussed.

II. THEORETICAL METHODS

We use spin-polarized density functional theory (SDFT) within the local spin density approximation (LSDA) to determine total energies, forces, and structural optimizations.[58,59] *Unconstrained* SDFT calculations—as well as *constrained* SDFT calculations with fixed spin moment[60]—are performed, depending on what is necessary. In unconstrained SDFT calculations, the total magnetic moment of the system is allowed to vary (i.e., unconstrained) during the charge self-consistent calculations, and a converged solution yields an optimized magnetic moment for a given atomic configuration. While unconstrained SDFT calculations are powerful to search for the ground state of the electron system with optimal magnetic moment, it does not directly produce the insight regarding the energy profile

corresponding to different magnetic moments. This insight can be obtained by constrained SDFT calculations, in which the total magnetic moment $|\mathbf{M}|$ is fixed during the charge self-consistent calculation, and then in a separate step, $|\mathbf{M}|$ is varied in order to find the total energies corresponding to different total magnetic moments.[60] All calculations in this study were performed using Quantum Espresso.[61]

We use the Troullier-Martins type[62] of norm-conserving pseudopotentials to describe the interaction between core electrons and valence electrons, with Ti $3s$ and $3p$ semicore states treated as valence states in order to improve accuracy and transferability.[63] Our pseudopotentials yield for bulk $BaTiO_3$ the correct energetics for different phases as well as a good bulk phonon dispersion. Furthermore, the theoretical strain-induced frequency shifts of non-soft phonon modes are in excellent agreement with experiments.[64] A large energy cutoff of 80 Ryd is used for all supercell calculations with vacancies, which provides sufficient convergence.

Our previous studies have shown that different ferroelectric phases in $BaTiO_3$ have negligible effects on the vacancy-induced properties such as vacancy formation energy and electronic structure,[65] since the c/a tetragonality is very small in $BaTiO_3$. Here we choose to study the tetragonal ($P4mm$) structure of $BaTiO_3$. Our calculated bulk $BaTiO_3$ with tetragonal symmetry has a in-plane lattice constant $a = 3.928$Å and a c/a ratio of 1.007, which are close to the values from other calculations (such as $a = 3.945$Å and c/a=1.009 in Ref.66), and are also comparable, within a typical LDA error, to the experimental values[67] ($a = 3.9945$Å and $c/a = 1.0098$).

To simulate vacancies in $BaTiO_3$, we use $3\times3\times3$ supercells with 135 atoms in order to reduce the interaction among vacancies, and one vacancy is placed at the center of each supercell. The $3\times3\times3$ supercell is sufficient and gives converged results. As a standard approach to study charged vacancies, a uniform jellium charge is utilized to avoid the Coulomb divergence for charged periodic systems.[45,46] Contribution by the uniform jellium charge to the total energy was shown in Ref.50. To handle the possible occurrence of partially occupied defect states introduced by vacancies, a smearing technique of Marzari and Vanderbilt was used.[68] A $\mathbf{k}$-point grid of $4\times4\times4$ Monkhorst-Pack sampling is used,[69] which is well converged considering that we are using a large supercell for vacancy calculations. For each vacancy species and each charge state considered in this study, atomic positions are fully relaxed before other properties are investigated. The force tolerance for optimization of atomic positions is 10^{-4} Ryd/Bohr.

III. RESULTS AND DISCUSSIONS

A. Dependence of magnetism on charge state

The stability of a magnetic state to be caused by vacancies is determined by calculating the energy difference $\Delta E = E_{GS} - E_{NM}$ between the total energy of the ground state, E_{GS}, and that of the non-magnetic state, E_{NM}. For each charge state of each vacancy species, we have performed *independently* two sets of calculations: structural optimization using unconstrained *spin-polarized* calculations (which yields the ground state, its energy E_{GS}, and optimal magnetic moment $|\mathbf{M}|$), and structural optimization using spin *non-polarized* calculations (which will yield only a non-magnetic state and its energy E_{NM}). Depending on the magnitude $|\mathbf{M}|$ of magnetic moment and the sign of ΔE, three types of ground states can be determined: (a) If $|\mathbf{M}| \neq 0$, the ground state of the system is ferromagnetic. Meanwhile, ΔE should be negative since the non-magnetic state is not the ground state and should thus have a higher energy. (b) If $|\mathbf{M}| = 0$ and $\Delta E < 0$, the ground state is antiferromagnetic (AFM), for the system has zero magnetic moment but non-magnetic state is not the ground state. (c) If $|\mathbf{M}| = 0$ and $\Delta E = 0$, the ground state of the system is non-magnetic.

We have computed the energy difference ΔE and the optimal magnitude $|\mathbf{M}|$ of magnetic moment for different vacancy species and different charge states in BaTiO$_3$, and results are given in Table I. In tetragonal BaTiO$_3$, there are two inequivalent oxygen sites by symmetry, and to distinguish them, we use O1 to denote an oxygen atom at the apex of an oxygen octahedron, and O2 to denote an oxygen atom on a TiO$_2$ base plane. Table I includes the results for both V_{O1}^q and V_{O2}^q vacancies.

Table I reveals the following key outcomes: (i) Vacancies V_{O1}^0, V_{O2}^0, V_{Ti}^q ($q = 0, 1-, 2-, 3-$), and V_{Ba}^0 all have non-zero optimal magnetic moment $|\mathbf{M}|$ (see the fourth column of Table I), thus possessing a ferromagnetic ground state. Furthermore, for these vacancies, ΔE is indeed negative as it should be. Note that the above vacancies with non-zero $|\mathbf{M}|$ include Ba vacancies (V_{Ba}^0), Ti vacancies (V_{Ti}^q), and O vacancies (V_{O1}^0 and V_{O2}^0). Our calculations thus predict that *all three vacancy species are able to induce ferromagnetism* in BaTiO$_3$. (ii) V_{Ti}^{3-}-induced FM state is found to be very stable with respect to the non-magnetic state, with an energy difference $\Delta E = -6.9$ meV and a large magnetic moment of $1.0\mu_B$ per vacancy. Other charge states of the same Ti vacancy species, such as V_{Ti}^{2-}, V_{Ti}^{1-}, and V_{Ti}^0 in Table I, have even larger magnetic moments. In contrast, the magnetic moments of V_{O1}^0 or V_{O2}^0 is considerably less, with only $0.25\mu_B$ per vacancy and with ΔE=-0.5 meV. We thus see that ferromagnetism caused by different vacancies behaves markedly different. (iii) No vacancies in Table I have simultaneously a zero magnetic moment and a negative ΔE, which is required by the antiferromagnetism. AFM is thus found not stable in BaTiO$_3$ with vacancies. In fact, we have performed additional calculations to investigated the possibility of the AFM state, by using different initial AFM configurations in the unconstrained searching. After optimization, the system always relaxes to either ferromagnetic or non-magnetic state, and we did not find that AFM is stable.

It is known that a system might be stuck at a metastable state in unconstrained spin-polarized DFT calculations, and then there is risk that the obtained solution is not the true ground state. To further ensure that the magnetic states found in Table I are indeed the ground state, rather than a metastable state, we have performed for each vacancy and each charge state a separate set of calculations using the constrained-moment approach[60], in which the structural optimization is first carried out within a subspace of a fixed total magnetic moment $|\mathbf{M}|$, and then $|\mathbf{M}|$ is varied to cover the full degrees of freedom. The results of constrained-moment calculations are shown in Fig.1 for the two vacancies with small ΔE—V_{O1}^0 and V_{Ba}^0; these two vacancies thus require more caution in identifying their ground states. Fig.1(a) shows that the energy minimum for V_{O1}^0 is located at $|\mathbf{M}| = 0.25\mu_B$, in excellent agreement with the result in Table I obtained from the unconstrained optimization. Interestingly, for V_{Ba}^0 in Fig.1(b), there are two local energy minima, one at $|\mathbf{M}| = 0.25\mu_B$ and the other at $|\mathbf{M}| = 1.0\mu_B$. The latter is the global minimum by having a slightly lower energy, again agreeing well with the result in Table I. Our constrained-moment calculations thus confirm that the magnetic states in Table I are indeed the ground state.

Obviously different vacancies occur in solid under different growth conditions. To evaluate under what condition vacancies V_{O1}^0, V_{O2}^0, V_{Ti}^{3-}, V_{Ti}^{2-}, V_{Ti}^{1-}, V_{Ti}^0, and V_{Ba}^0 (i.e., those vacancies that yield FM in Table I) may occur in BaTiO$_3$, we go one step further and have determined the formation energies of various vacancies, again using first-principles density functional calculations. The results are given in the Appendix. The calculation results in the Appendix show that, under the oxygen-rich condition, the formation energies of cation vacancies V_{Ba}^0, V_{Ti}^{3-}, V_{Ti}^{2-}, V_{Ti}^{1-}, and V_{Ti}^0 are reasonably small (below 4 eV) when the chemical potential μ_e of the electron reservoir is below 1eV. Therefore, V_{Ba}^0, V_{Ti}^{3-}, V_{Ti}^{2-}, V_{Ti}^{1-}, and V_{Ti}^0 are likely to occur in BaTiO$_3$ under the O-rich condition. Meanwhile, the Appendix also shows that, under the oxygen-poor condition, the formation energy of V_{O1}^0 is merely 1.33 eV, which is small. V_{O1}^0 is thus highly possible under the O-poor condition.

Our theoretical results are consistent with available experimental observations. In experiment, oxygen deficient BaTiO$_3$ thin films were prepared by pulsed laser deposition, and magnetic hysteresis loops were clearly observed,[40] revealing the existence of ferromagnetism in BaTiO$_3$ with oxygen vacancies. Furthermore, when samples were annealed in 1 atm of oxygen (to remove oxygen vacancies), the magnetism disappears.[40] This is consistent with, and can be explained by, our theoretical result that V_O^0 is able to induce ferromagnetism.

Here it worths pointing out that not every BaTiO$_3$ sample with oxygen deficiency exhibits magnetism. According to our theory, two conditions are needed in order for oxygen vacancies V$_O^q$ to be magnetic: (i) An oxygen poor condition is needed so that the formation energy of V$_O^q$ is low and oxygen vacancies can exist (as shown in the Appendix); (ii) The charge state q of V$_O^q$ need be neutral, since only neutral V$_O^0$ is magnetic according to our calculation results in Table I. Condition (ii) means that V$_O^0$ need be more stable than V$_O^{1+}$ and V$_O^{2+}$, which indicates that the chemical potential μ_e of the electron reservoir shall be near the conduction band minimum (CBM) (see the Appendix for details). As a result, not every BaTiO$_3$ with oxygen deficiency exhibits magnetism.

Our finding that all three vacancy species can induce ferromagnetism in BaTiO$_3$ is of important relevance. First, the result reveals that ferromagnetism can occur under either oxygen-rich or oxygen-poor condition. Under oxygen-rich condition, V$_{Ba}^0$ or V$_{Ti}^0$ vacancies are the possible cause of FM, since these vacancies are most likely to occur when oxygen is rich. Under oxygen-poor condition, V$_{O1}^0$ or V$_{O2}^0$ vacancies are the possible cause. The finding may also allow scientists to tune the growth condition and generate deliberately a certain species of vacancies so that magnetism induced by different vacancy species can be studied and contrasted. Furthermore, in experiments, V$_O$ is commonly assumed to be the cause of induced magnetism[40,41]. This need be taken with caution according to our calculations. For instance, if FM is caused by V$_{Ti}^{3-}$, assuming that it is caused by V$_O^0$ will lead to an incorrect understanding of the origin of magnetism.

Besides the above results, our study also provides other pivotal knowledge. As a matter of fact, three interesting and generally applicable observations can be made from Table I: (1) The induced magnetism depends critically on the charge state of the vacancy. For instance, V$_{O1}^q$ can induce magnetism only when $q=0$, and in contrast, V$_{O1}^{2+}$ and V$_{O1}^{1+}$ are non-magnetic (Table I). This marked dependence of magnetism on q is even more dramatic for Ti vaccancies. For V$_{Ti}^q$, the magnetic moment varies drastically for different charge states q, ranging from $|\mathbf{M}|=1.0\mu_B$ at $q=3-$ to $|\mathbf{M}|=3.50\mu_B$ at $q=0$. The sensitive dependence of vacancy-induced magnetism on the charge state clearly demonstrates that one must examine different charge states in order to obtain a better and complete understanding of the topic.

(2) We notice that V$_{O1}^{1+}$, V$_{O2}^{1+}$, and V$_{Ba}^{1-}$ all have an odd number of electrons per supercell. According to conventional wisdom, systems with an odd number of electrons tend to be spin-polarized, since spin-up and spin-down electrons are unbalanced. Our first-principles results in Table I show that this is not true for vacancy-induced magnetism: V$_{O1}^{1+}$, V$_{O2}^{1+}$, and V$_{Ba}^{1-}$ turn out to be non-magnetic. The results also tell that, for a given charge state, one should not rely on counting the number of electrons to determine whether or not magnetism exists.

(3) Interestingly, the nominal charge states of three vacancy species (i.e., V$_{Ba}^{2-}$, V$_{Ti}^{4-}$, and V$_O^{2+}$ in Table I) do not induce magnetism. Here, the nominal charge state means that the vacancy carries a charge q which is *opposite* to what an ion of the same species would carry in a perfect solid. For instance, in perfect bulk BaTiO$_3$, an O ion carries a charge amount of 2-, with two additional electrons transferred from the neighboring cations. By definition, the nominal charge state of V$_O$ will be 2+. The nominal charge state is important since it is the state commonly anticipated to occur for a given vacancy species. Consider an oxygen vacancy as an example. When we create an oxygen vacancy by taking one O atom out of the bulk solid (this O atom is to be called "O^{out}") and placing O^{out} into the oxygen atomic reservoir, the two additional electrons of O^{out} (which are transferred from neighboring cations) have a tendency to follow O^{out} because it is energetically favorable for these two electrons to be bound to O^{out} due to the strong electronegativity of oxygen. This will lead to the solid carrying an opposite $q=2+$ charge state (i.e., V$_O^{2+}$). Therefore, the nominal charge state of an oxygen vacancy is V$_O^{2+}$. Similarly, the nominal charge state is V$_{Ba}^{2-}$ for Ba vacancies, and V$_{Ti}^{4-}$ for Ti vacancies.

The finding that the nominal charge state is non-magnetic is intriguing, which is difficult to explain. Here we try to provide an intuitive explanation within a tight-binding model. We recognize that this is only an approximate model, but it will not affect our overall conclusion. In perfect bulk BaTiO$_3$, atomic orbitals of each ion can be approximately treated as closed-shell, i.e., either fully occupied or fully empty, due to strong charge transfer in this solid. Now, in BaTiO$_3$ with V$_O^{2+}$, since the two additional electrons surrounding the O^{out} atom are taken out of the solid, the atomic-orbit shells of the neighboring Ti and Ba atoms next to O^{out} remain closed-shell, which bears an interesting resemblance to the perfect solid and thus leaves no charge for spin polarization (therefore $|\mathbf{M}|=0$).

We have further examined whether our conclusions about the existence of magnetism are to be altered if the LDA band gap is corrected by, e.g., more accurate density functional. Ideally one would prefer to perform calculations using the Heyd-Scuseria-Ernzerhof (HSE) screened hybrid functional,[70] which yields in general correct band gaps for various solids. It turns out that HSE hybrid-functional calculations for large supercells of 135 atoms are prohibitively time consuming. We thus decide to perform LDA+U calculations with different U to achieve correct band gaps, and to investigate how magnetic moment $|\mathbf{M}|$ may be affected. The on-site Coulomb interaction U is added on Ti atoms. Here we will mainly consider V$_{O1}^0$ and V$_{Ti}^{3-}$, since the former is the key vacancy that generates magnetism under O-poor condition, and the latter is the key vacancy that generates magnetism under O-rich condition. We find that, for V$_{O1}^0$, the calculated magnetic moment $|\mathbf{M}|$ is 0.25, 0.5, 1.5 μ_B for U=0, 3, 6 eV, respectively. For V$_{Ti}^{3-}$, $|\mathbf{M}|$ is obtained as 1.00, 0.93, 0.56 μ_B for U=0, 3, 6 eV, respectively. U values between 3eV and 6eV have been used in the literature for perovskite oxides,[71,72] which produce theoretical band gaps similar

to the experiment values. We see that, at U=6eV, both V_{O1}^0 and V_{Ti}^{3-} are still ferromagnetic, and our conclusions thus largely remain.

We have also examined how different theories (LDA, or LDA+U with different U) may affect the defect levels of V_{O1}^0 in BaTiO$_3$. Previously it was reported that, in another perovskite SrTiO$_3$, the defect levels of neutral oxygen vacancies are rather complex, depending sensitively on what theory (LDA or LDA+U) is used.[73] We find that the results in BaTiO$_3$ bear some similarity to those in SrTiO$_3$, but also show difference. Within LDA, the defect states of V_{O1}^0 in BaTiO$_3$ are found to be located inside the conduction band (i.e, forming a band resonance), much like[73] SrTiO$_3$. When LDA+U is employed, our calculations reveal that, for small U (e.g., U=3 eV), the defect states of V_{O1}^0 are still resonant within the conduction band. As U is increased to 6 eV (which is a typical value used in the literature for Ti atoms), a defect state appears inside the band gap. However, unlike SrTiO$_3$ where the defect state is a deep level ($\sim$0.7 eV below the conduction-band edge[73]), the defect state of V_{O1}^0 in BaTiO$_3$ is rather shallow and located about 0.20 eV below the conduction-band edge.

The difference between SrTiO$_3$ and BaTiO$_3$ in terms of their sensitivity of defect levels to the U value may be explained to some extent by the fact that SrTiO$_3$ is an incipient ferroelectric (namely this material is on the edge of becoming ferroelectric, but is not yet ferroelectric). As an incipient ferroelectric near the paraelectric-ferroelectric phase boundary, SrTiO$_3$ has an exceptionally large low-temperature dielectric constant (on the order of 10^4 depending on orientation), and its structural properties were shown in Ref.72 to be sensitive to U since different U values lead to very different dielectric screening. Therefore, for SrTiO$_3$, LDA+U with large U gives rise to large changes in atomic relaxation and defect levels. In contrast, BaTiO$_3$ is a ferroelectric (i.e., this solid is away from the paraelectric-ferroelectric phase boundary), and its dielectric screening is less sensitive to U than SrTiO$_3$. As a result, the defect level of V_{O1}^0 in BaTiO$_3$ undergoes a smaller change even at large U, leading to a shallow defect state within the band gap.

B. Origin of ferromagnetism

The result in Sec.IIIA that both cation vacancies (V_{Ba}, V_{Ti}) and anion vacancies (V_{O1},V_{O2}) can induce FM in BaTiO$_3$ is rather remarkable, since, according to the theory of semiconductor physics,[74] these two types of vacancies should have very different electronic properties. It is thus interesting to understand what cause the magnetisms for cation vacancies and for anion vacancies. Do they come from the same mechanism? What difference may exist between cation-induced FM and anion-induced FM? We next attempt to provide the origin of magnetism from two different aspects: one is from the *energy* space, and the other from the spin density in *real space*.

We begin with the energy space by examining the spin-resolved densities of states (DOS) near the Fermi level E_F, which are plotted in Fig.2 for those vacancies that are able to induce magnetism. For non-magnetic V_{Ba}^{2-}, V_{Ti}^{4-}, and V_{O1}^{2+}, the calculated spin-up and spin-down DOS components (not shown) are identical, resulting in a vanishing magnetic moment.

For cation vacancies V_{Ti}^{3-}, V_{Ti}^{2-}, and V_{Ba}^0, Fig.2(b)-(d) show that (i) the Fermi levels (E_F) are located inside the *valence* states, revealing that for these vacancies we are dealing with acceptors where carriers are holes. (ii) By focusing on the valence states, it is evident that the spin-up and spin-down DOS components are asymmetric, with spin-up component subject to an observable downshift toward lower energies compared to the spin-down component [see, e.g., Fig.2(b)]. In other words, the valence states are clearly spin polarized. (iii) However, and interestingly, this is not the case for the *conduction* states, in which the up and down DOS components remain nearly identical [again, see Fig.2(b)]. We thus find that, for V_{Ba}^0, V_{Ti}^{2-}, and V_{Ti}^{3-} vacancies, the spin polarization occurs mainly to the valence states, but not to the conduction states. The results (i)-(iii) demonstrate that ferromagnetism induced by the cation vacancies is caused by the spin polarization of *holes*.

However, for anion vacancy V_O^0, Fig.2(a) shows drastically different behaviors. For V_{O1}^0, E_F is now located inside the conduction states. Therefore, with V_O^0 vacancies we are dealing with a donor with electrons being the carriers, unlike cation vacancies. Furthermore, in Fig.2(a), the conduction states are spin polarized while the valence states are nearly not, revealing that FM induced by V_O^0 is caused by the spin polarization of *electrons*. Also interestingly, note in Fig.2(a) that, for conduction states, the energy shift of the spin-up DOS component with respect to the spin-down component is barely perceptible, and is much smaller compared to the energy shift of the valence states in Fig.2(b). This explains why V_{Ti}^{3-} has a lower $\Delta E = E_{GS} - E_{NM}$ and thus stronger magnetic instability than V_{O1}^0 in Table I.

The finding in Fig.2—that FM is caused by spin polarization of holes for cation vacancies, but by spin polarization of electrons for anion vacancies—could be very helpful in engineering FM in FEs. Note that, in Fig.2(b) for cation vacancies, when energy E is decreased from E_F, the DOS of valence states increases substantially. It suggests that, if holes are doped into BaTiO$_3$ with cation vacancies so that E_F is pushed down, there will be more valence states near E_F that are spin-polarized, by using first-order perturbation theory that the electron states are largely unchanged by doping except E_F is moved. Therefore $|\mathbf{M}|$ will increase after hole doping. This intriguing observation is indeed confirmed by our calculation results on V_{Ti}^{2-}. Compared to V_{Ti}^{3-}, V_{Ti}^{2-} has a less negative charge (thus is doped with hole), and the first-principles calculations in Table I show that V_{Ti}^{2-} indeed has a larger magnetization, consistent with the above argument. Similarly, it is easy to understand that for anion

vacancies V_O, doping with electrons will likely increase the magnetization.

We now investigate another key issue concerning whether magnetism induced by vacancies is localized or delocalized, so that more microscopic insight responsible for the magnetism can be obtained. For this purpose, we study the real-space spin density $\Delta\rho(\mathbf{r}) = \rho_\uparrow(\mathbf{r}) - \rho_\downarrow(\mathbf{r})$, which is depicted in Fig.3(a)-(d). The contours in Fig.3 are on a XZ plane that cuts through the vacancy; a XZ plane is parallel to an ac plane in tetragonal bulk BaTiO$_3$. A plane cutting through the vacancy is chosen so we can examine the spin density $\Delta\rho(\mathbf{r})$ near the vacancy.

For V_{O1}^0, two important conclusions can be obtained from Fig. 3(a). First, the spin density is distributed mainly on the Ti atoms, and exhibits a shape of t_{2g} orbital, showing that magnetization is contributed by the unbalanced spin-up and spin-down occupations on the Ti t_{2g} orbitals. This can be explained by the fact that V_{O1}^0 has two excessive electrons compared to V_{O1}^{2+}, and these additional electrons must be placed on the low-energy conduction states that are mainly Ti $3d$ orbitals, thereby leading to the shape of the spin-polarized density in Fig 3(a). Second, and rather remarkably, the spin density in Fig.3(a) is spreading over the entire supercell. In other words, our calculations show that $\Delta\rho(\mathbf{r})$ is *not* localized near the vacancy. The delocalized nature of the spin density reveals an important conclusion, that is, the V_O^0-induced ferromagnetism in BaTiO$_3$ is due to itinerant electrons.

Interesting differences arise when we examine cation vacancies (V_{Ti}^{3-}, V_{Ti}^{2-}, and V_{Ba}^0). For these cation vacancies, Fig.3(b)-(d) reveal: (i) The spin polarization occurs on the O atoms, unlike anion vacancies where $\Delta\rho(\mathbf{r})$ is on the Ti sites. (ii) The shape of $\Delta\rho(\mathbf{r})$ at the O sites manifests that it is mainly the O $2p$ orbitals that are spin-polarized (see, e.g., Fig.3b). This can be easily understood if we begin with the nominal charge state such as V_{Ti}^{4-} (or V_{Ba}^{2-}), in which the valence orbitals of all atoms (including the O $2p$ orbitals near vacancy) are close-shelled as described in Sec.IIIA. Now with the charge state V_{Ti}^{3-} (or V_{Ba}^0), *less* electrons exist in the system compared to V_{Ti}^{4-} (or V_{Ba}^{2-}, respectively), thereby creating holes near the top of valence bands which mainly comprise of the $2p$ states of the O atoms. This explains why the spin density in Fig.3(b)-(d) is mainly at O sites with $2p$-like shape. It also highlights the conceptual importance of the nominal charge state in terms of understanding the magnetic behaviors of vacancy-induced magnetism. (iii) Similar to anion vacancies, $\Delta\rho(\mathbf{r})$ of cation vacancies also spreads out in the supercell.

Our results in Fig.3 shed new light on the vacancy-induced magnetism. According to our calculations, the spin density $\Delta\rho(\mathbf{r})$ is widespread in real space. This is in sharp difference from the previous knowledge[49,55] reported in the literature. Previously the spin density induced by an oxygen vacancy in PbTiO$_3$ was determined, and $\Delta\rho(\mathbf{r})$ was found to be very localized, which is dis-

tributed within the nearest neighbor of the vacancy.[49,55] These previous studies showed that vacancy-induced magnetism originates from highly localized magnetic moments. In contrast, our calculations show that the spin density induced by V_O in BaTiO$_3$ is delocalized, and spreads as far as the fifth neighbors of the vacancy (Fig.3a), which demonstrates a different origin of magnetism, namely the magnetism stems from itinerant electrons. One possible reason for this discrepancy is the size of supercell: a $2 \times 2 \times 2$ supercell was used[49,55] for PbTiO$_3$. We find that a $3 \times 3 \times 3$ supercell is needed in order to obtain the correct spreading of $\Delta\rho(\mathbf{r})$. We have performed calculations using a $2 \times 2 \times 2$ supercell, and found that $\Delta\rho(\mathbf{r})$ is rather localized, similar to that obtained in Ref.55.

Combining the results in Fig.2 and Fig.3, we thus see that the magnetism of oxygen vacancies originates from the spin polarization of the itinerant electrons at Ti t_{2g} orbitals. The itinerant theory of magnetism also applies to the cation vacancies in BaTiO$_3$, but we need to think in term of the delocalized holes. More specifically, ferromagnetism of V_{Ti}^{3-}, V_{Ti}^{2-}, and V_{Ba}^0 is attributed to the spin polarization of itinerant holes at O $2p$ orbitals.

C. Temperature range for magnetism

The temperature range that ferromagnetism can sustain is important in terms of potential technological applications. For instance, ferromagnetism existing at room temperature or even higher is desirable for magnetic and spintronics devices, so that the energy-costing process of cooling is not needed. Different vacancy species generate very different local interactions, which leads to a new balance of various interactions around the defect. It is thus interesting to investigate which vacancy-induced magnetic moment may sustain high temperatures. For this purpose, ideally one would prefer to perform *finite-temperature* DFT calculations, which is computationally prohibitive for large supercells. However, considering that the temperature range of magnetism is an important quantity, even a less accurate evaluation will be very useful. Here, we decide to use a tractable and effective approach to determine the temperature range that magnetism can survive. Since magnetism induced by vacancies in BaTiO$_3$ has an itinerant origin, the main effect of temperature is to change the population of electron states. We thus vary the smearing width σ in the calculations of spin-polarized band structure and magnetic moment, to mimic the effect of temperature. The obtained magnetic moments are shown in Fig.4 as a function of smearing width σ for V_{O1}^0, V_{Ti}^{3-}, and V_{Ba}^0.

One general observation, which is applicable to all three vacancies, can be made by examining the three $|\mathbf{M}| \sim \sigma$ lineshapes in Fig.4(a)-(c). That is, the magnetic moment saturates at low σ, then starts to decline, and eventually vanishes at high σ. This general behavior is no accident, and can be intuitively explained us-

ing a simple two-level system that is to be occupied by one electron. The two levels are separated by an energy difference Δ due to spin polarization. According to the Fermi-Dirac distribution, when thermal excitation energy (k_BT) is much smaller than the energy separation Δ (i.e., $k_BT << \Delta$), only one level is occupied, leading to spin polarization and a nonzero magnetic moment. This explains the saturated magnetization at low σ (i.e., the low-temperature limit) in Fig.4. On the other hand, in the high-temperatures limit which satisfies $k_BT >> \Delta$, thermal excitation will make both levels occupied, resulting in a diminished magnetic moment and a spin non-polarized system. It explains why $|\mathbf{M}|$ disappears at high σ in Fig.4.

There are, however, important differences among the three curves in Fig.4. In Fig.4(a) for V_{O1}^0, we see that $|\mathbf{M}|$ vanishes when σ is above 10 meV; this critical σ value is to be denoted as σ_c. In other words, above $\sigma_c=10$ meV (which corresponds to a temperature of $\sim$120K), the magnetic moment of V_{O1}^0 becomes virtually null. Now compare the critical σ_c value of V_{O1}^0 (Fig.4a) with that of V_{Ti}^{3-} (Fig.4b) and of V_{Ba}^0 (Fig.4c), and we find that σ_c drastically differs for different vacancies. More specifically, ferromagnetism of V_{Ti}^{3-} can exist at considerably larger σ, up to $\sigma_c=113$ meV, indicating that FM of Ti vacancies sustains at a much higher temperature ($\sim$1300 K). The magnetism caused by Ti vacancies is thus promising for room-temperature magnetic and spintronic applications. For V_{Ba}^0, Fig.4(c) shows that its magnetism can survive up to $\sim$370 K. Our study thus predicts that the temperature range of magnetism depends critically on which vacancy species is created.

Based on our theoretical result that V_{Ti}^{3-} vacancies generate a much larger magnetic moment ($1\mu_B$) than V_O^0 ($0.25\mu_B$), we suggest that preparing BaTiO$_3$ in oxygen-rich environment (so that V_{Ti}^{3-} vacancies may occur) may produce an even stronger ferromagnetism. Moreover, the ferromagnetism of V_{Ti}^{3-} may exist at and above the room temperature, which is attractive for spintronic and multiferroic devices.

We further numerically find that the lineshapes of the three $|\mathbf{M}|$-vs-σ curves in Fig.4 can be universally described by an analytic formula $|\mathbf{M}| = \frac{|\mathbf{M}|_0}{1+e^{(\sigma-\sigma_0)/d}}$, where $|\mathbf{M}|_0$ is the saturated magnetic moment at low temperature, σ_0 is the characteristic transition point where $|\mathbf{M}|$ decreases to half of the saturated $|\mathbf{M}|_0$ value, and d is the width. A larger σ_0 indicates a higher temperature which magnetism can sustain. Analytic fitting of the above formula to the direct calculation results produces $|\mathbf{M}|_0$, σ_0, and d to be respectively $0.25\mu_B$, 7.46 meV, and 0.84 meV for V_{O1}^0; $1.0\mu_B$, 83.7 meV, and 9.68 meV for V_{Ti}^{3-}; and $1.0\mu_B$, 23.1 meV, and 2.03 meV for V_{Ba}^0. The saturated $|\mathbf{M}|_0$ values agree well with the direct first-principles results in Table I. The σ_0 value of V_{Ti}^{3-} is large, consistent with the fact that its magnetism can sustain at high temperature.

IV. SUMMARY

Magnetism caused by native vacancies in ferroelectric BaTiO$_3$ is a topic of fundamental interest, and was investigated here using first-principles density functional calculations. We have examined various properties, including which vacancy species may give rise to magnetism, the influence of charge state on induced magnetic moment and on the energetics of magnetic instability, the microscopic origin responsible for the emergence of magnetism, as well as the temperature range that magnetism may sustain. The present study not only provides a rather comprehensive understanding on vacancy-induced magnetism in ferroelectrics, it also sheds new light on several key issues that are previously unsettled. Furthermore, this study yields some useful guide on how to control the magnetism by selectively controlling which vacancy to appear under a certain growth condition (see Appendix). Our specific findings are summarized in the following.

(i) Ferromagnetism in BaTiO$_3$ can be induced by native vacancies V_{Ba}^0, V_{Ti}^q ($q = 3-, 2-, 1-, 0$), and V_O^0. Our calculations show that these vacancies all possess a significant nonzero ferromagnetic moment. The existence of ferromagnetism is confirmed by unconstrained DFT calculations as well as by constrained-moment calculations. This result reveals that, even under oxygen-rich condition in which V_O vacancies are unlikely to form, it is still possible that FM may exist in BaTiO$_3$, and this FM will be caused by V_{Ba}^0 or by V_{Ti}^q. In fact, according to our calculations, the magnetic moment and magnetic instability are predicted to be very strong for V_{Ti}^q vacancies when q is $3-, 2-, 1-$, and 0. Furthermore, antiferromagnetism is found not stable in BaTiO$_3$.

(ii) The charge state of vacancy, which has been overlooked in the existing studies on vacancy-induced magnetism, is found pivotal in terms of determining the stability of the FM phase and in determining the magnetic moment of vacancy. We showed that V_O^{2+} and V_O^{1+} are non-magnetic, whereas V_O^0 is FM. Also, the magnetic moments of V_{Ti}^0 and V_{Ti}^{3-}, two different charge states of the same vacancy species, are found to differ drastically; $|\mathbf{M}|$ is $3.5\mu_B$ for the former, but is much less ($1.0\mu_B$) for the latter. These results point to a conclusion that we must consider different charge states when studying vacancy-induced magnetism. Also interestingly, we found that the nominal charge states is non-magnetic, and this general rule is shown to be correct for all three vacancy species. Moreover, our study demonstrates that the naive approach of judging vacancy-induced magnetism by counting the number of electrons is unjustified.

(iii) We have investigated the origin of magnetism in BaTiO$_3$ from both the energy space and the real space. The origin is shown to be different for cation-vacancies induced FM and for anion-vacancies induced FM. Ferromagnetism induced by V_O^0 vacancies originates from the spin polarization of itinerant electrons in the *conduction* states. The spin density is predominately located at Ti

t_{2g} orbitals. Interestingly, the *valence* states are nearly spin non-polarized for V_O^0 vacancies.

On the other hand, magnetism induced by V_{Ti}^{3-} and V_{Ba}^0 is caused by the spin polarization of itinerant *holes*, and the spin density is mainly located at O $2p$ orbitals. Based on the finding that FM of cation vacancies is caused by itinerant holes, we further suggest that hole doping can effectively increase the magnetic moment of cation vacancies. This is indeed confirmed by our calculations when we contrast V_{Ti}^{2-} with V_{Ti}^{3-}. Compared to V_{Ti}^{3-} with $|\mathbf{M}|=1.0\mu_B$, V_{Ti}^{2-} has more hole in the system, and its magnetic moment increases to $|\mathbf{M}|=1.52\mu_B$.

Moreover, for both cation and anion vacancies, we found that the spin densities of vacancy-induced magnetism are spread, which is in difference from the previous studies where $\Delta\rho$ was localized near the vacancy.

(iv) The temperature range of ferromagnetism is shown to differ drastically for different vacancy species. FM of V_O^0 exists only at relatively low temperatures. But magnetism of V_{Ti}^{3-} can survive at very high temperatures ($\sim$1300K). FM of V_{Ti}^{3-} is thus promising for room-temperature magnetic and spintronic applications. We further showed that the $|\mathbf{M}|$-vs-σ lineshapes of all three vacancy species in Fig.4 follow a universal analytic formula.

V. APPENDIX

In this Appendix we investigate under what condition vacancies V_{O1}^0, V_{O2}^0, V_{Ti}^{3-}, V_{Ti}^{2-}, V_{Ti}^{1-}, V_{Ti}^0, or V_{Ba}^0 (i.e., those vacancies which cause FM in Table I) may occur in BaTiO$_3$. This knowledge may also be useful to experimentalists on how one could control the magnetism by selectively controlling which vacancy species to appear in BaTiO$_3$ solid, using the chemical potentials of atomic reservoirs and the chemical potential of electron reservoir. Quantitatively, the concentration of vacancies V_X^q is determined by the formation energy, which is defined as[45,46]

$$\Delta H[V_X^q] = E(V_X^q) + \left[\mu_X + E_X^0\right] + q\left[\mu_e + \varepsilon_{VBM}^0 + \Delta\overline{V}\right] - E(ABO_3), \tag{1}$$

where $E(V_X^q)$ is the total energy per supercell of the defective solid with vacancies V_X^q, $E(ABO_3)$ the total energy of a perfect solid, E_X^0 the total energy per atom of an elemental solid of species X, ε_{VBM}^0 the single-particle orbital energy of the valence band maximum (VBM) of the perfect crystal, $\Delta\overline{V}$ the difference in the average potential between a perfect solid and the defective solid with V_X^q vacancies. μ_X is the chemical potential of atomic reservoir of species X. According to the convention of defect physics,[45,46] E_X^0 of the elemental solid is used here as the zero energy reference to define the chemical potential μ_X. μ_e is the chemical potential of the electron reservoir with respect to the VBM of the defective solid. In Eq.(1), the vacancy formation energy ΔH is controlled by chemical potentials μ_X and μ_e, which can be varied in experiments. The rational of Eq.(1) and how each term is calculated using DFT were explained in Ref.50.

It is known[45] that chemical potential μ_X must satisfy thermodynamic constraints in order to avoid the formation of (unwanted) secondary phases [such as BaO and TiO$_2$ compounds or elemental solids] during growth. For BaTiO$_3$, the details of these thermodynamic constraints were described in Ref.65. Here we recalculate these constraints using Quantum Espresso. The obtained constraints are -7.39 eV $\leq \mu_{Ba} + \mu_O \leq$ -5.70 eV; -12.13 eV $\leq \mu_{Ti} + 2\mu_O \leq$ -10.44 eV; $\mu_{Ba} \leq 0$; $\mu_{Ti} \leq 0$; and $\mu_O \leq 0$. These results are close to those in Ref.65; the latter were obtained using a mixed-basis DFT code. For instance, for a given μ_O, the energy width Δ within which μ_{Ti} can vary is $\Delta = 1.69$ eV in the present calculation, in good agreement with $\Delta = 1.62$ eV in Ref.65.

In experiments, the chemical potential (μ_O) of the oxygen reservoir is often used to control the growth.[44] Here we simulate this experimental situation by allowing μ_O to vary, and μ_{Ba} and μ_{Ti} are then determined by the constraints accordingly using the middle point of each thermodynamical range, namely $\mu_{Ba} + \mu_O = -6.545$ eV and $\mu_{Ti} + 2\mu_O = -11.285$ eV. From the thermodynamic constraints, we find that μ_O can vary within the range $\mu_O \in [-5.7, 0]$ eV. We thus choose to consider two representative values of μ_O: μ_O=0 (which corresponds to the O-rich condition) and $\mu_O = -4$ eV (which is near the O-poor condition). At these two values of μ_O, the computed formation energies of different vacancies are shown in Fig.5.

Concentration $N[V_X^q]$ of vacancies V_X^q in solid depends on the formation energy $\Delta H[V_X^q]$ according to $N[V_X^q] = N_0 e^{-\Delta H[V_X^q]/k_BT}$, where N_0 is the number of atomic sites per unit volume. By measuring carrier concentration, the typical experimental value of V_O concentration was reported to be 8×10^{18} cm^{-3} in BaTiO$_3$,[22,23] while higher concentrations can reach[40,75] 4.53×10^{21} cm^{-3}. Using the typical experimental value of V_O concentration, we estimate that the formation energy of this vacancy is about 1 eV when sample is annealed at 1000 K. This estimation suggests that vacancies are easy to form when the vacancy formation energy is less than 1.5 eV. When formation energy is between 1.5 to 4 eV, vacancies are still likely to occur but with a decreased concentration. On the other hand, if formation energy is above 4 eV, vacancies are unlikely to form.

Fig.5 reveals the following: (i) Under the O-poor condition, and when μ_e is above 2 eV, V_{O1}^0 is the lowest-energy charge state with a low formation energy of 1.33 eV [see Fig.5(a)], and is thus easy to occur. As shown in Table I, V_{O1}^0 vacancies give rise to FM. (ii) Under the O-rich condition, and when μ_e is below 1eV, the formation energies of V_{Ti}^{4-}, V_{Ti}^{3-}, and V_{Ti}^{2-} are around 1.5eV and are quite close to each other [see Fig.5(e)], and these vacancies are thus likely to occur. Since V_{Ti}^{3-} and V_{Ti}^{2-} are ferromagnetic with strong FM instability (Table I), Fig.5(e) thus demonstrates that magnetism caused by Ti vacancies is

certainly possible in BaTiO$_3$. (iii) Under the O-rich condition and when μ_e is less than 0.5eV in Fig.5(f), the formation energy of V$_{\text{Ba}}^0$ is comparable to those of V$_{\text{Ba}}^{1-}$ and V$_{\text{Ba}}^{2-}$, and is around 2.8eV. Therefore V$_{\text{Ba}}^0$ is also possible in BaTiO$_3$, and will cause ferromagnetism. We thus

conclude, based on quantitative calculations, that those vacancy species which are FM (namely, V$_{\text{O1}}^0$, V$_{\text{Ti}}^{3-}$, V$_{\text{Ti}}^{2-}$, and V$_{\text{Ba}}^0$) are likely to occur when the chemical potentials μ_O and μ_e are properly chosen.

1 M. E. Lines and A. M. Glass *Principles and applications of ferroelectrics and related materials* (Clarendon Press, Oxford, 1977).

2 M. Dawber, K. M. Rabe, and J. F. Scott, Rev. Mod. Phys. **77**, 1083 (2005).

3 R. E. Cohen, Nature (London) **358**, 136 (1992).

4 R. E. Cohen and H. Krakauer, Phys. Rev. B **42**, 6416 (1990).

5 S.-E. Park and T.R. Shrout, J. Appl. Phys. **82**, 1804 (1997).

6 A. Garcia and D. Vanderbilt, Appl. Phys. Lett. **72**, 2981 (1998).

7 H. Fu and R.E. Cohen, Nature (London) **403**, 281 (2000).

8 A.M. George, J. Iniguez, and L. Bellaiche, Nature (London) **413**, 54 (2001).

9 Y.-K. Choi, T. Hoshina, H. Takeda, T. Teranishi, and T. Tsurumi, Appl. Phys. Lett. **97**, 212907 (2010).

10 J.B. Neaton and K.M. Rabe, Appl. Phys. Lett. **82**, 1586 (2003).

11 N. Sai, B. Meyer, and D. Vanderbilt Phys. Rev. Lett. **84**, 5636 (2000).

12 C.J. Fennie and K.M. Rabe, Phys. Rev. B **72**, 100103(R) (2005).

13 E. Bousquet, *et al.* Nature (London) **452**, 732 (2008).

14 N. Sai, C.J. Fennie, and A.A. Demkov, Phys. Rev. Lett. **102**, 107601 (2009).

15 N.A. Benedek and C.J. Fennie, Phys. Rev. Lett. **106**, 107204 (2011).

16 J.M. Rondinelli and C.J. Fennie, Adv. Mater. **24**, 1961 (2012).

17 S. E. Reyes-Lillo and K.M. Rabe, Phys. Rev. B **88**, 180102(R) (2013).

18 A.K. Tagantsev, K. Vaideeswaran, S.B. Vakhrushev, A.V. Filimonov, R.G. Burkovsky, A. Shaganov, D. Andronikova, A.I. Rudskoy, A.Q.R. Baron, H. Uchiyama, D. Chernyshov, A. Bosak, Z. Ujma, K. Roleder, A. Majchrowski, J.-H. Ko and N. Setter, Nat. Comm. 4, 2229 (2013).

19 I.I. Naumov, L. Bellaiche, and H. Fu, Nature (London) **432**, 737 (2004).

20 I. Naumov and H. Fu, Phys. Rev. Lett. **98**, 077603 (2007); X. Fu, I.I. Naumov, and H. Fu, Nano. Lett. **13**, 491 (2013).

21 I. Naumov and A. M. Bratkovsky, Phys. Rev. Lett. **101**, 107601 (2008).

22 C.N. Berglund and W.S. Baer, Phys. Rev. **157**, 358 (1966).

23 C.N. Berglund and H.J. Braun, Phys. Rev. **164**, 790 (1967).

24 B.A. Weschler and M.B. Klein, J. Opt. Soc. Am. B **5**, 1711 (1988).

25 J. F. Scott and M. Dawber, Appl. Phys. Lett. **76**, 3801 (2000).

26 M. Brazier, S. Mansour, and M. McElfresh, Appl. Phys. Lett. **74**, 4032 (1999).

27 S. Pöykkö and D. J. Chadi, Phys. Rev. Lett. **83**, 1231 (1999).

28 F. Yang, M. H. Tang, Y. C. Zhou, Fen Liu, Y. Ma, X. J. Zheng, J. X. Tang, H. Y. Xu, W. F. Zhao, and Z. H. Sun, Appl. Phys. Lett. **92**, 022908 (2008).

29 L. He and D. Vanderbilt, Phys. Rev. B **68**, 134103 (2003).

30 A.V. Kimmel, P.M. Weaver, M.G. Cain, and P.V. Sushko, Phys. Rev. Lett. **109**, 117601 (2012).

31 A. Chandrasekaran, D. Damjanovic, N. Setter, and N. Marzari, Phys. Rev. B **88**, 214116 (2013).

32 L. Bellaiche, J. Iniguez, E. Cockayne, and B.P. Burton, Phys. Rev. B **75**, 014111 (2007).

33 X. Ren, Nat. Mater. **3**, 91 (2004).

34 E. Cockayne and B. P. Burton, Phys. Rev. B **69**, 144116 (2004).

35 N. A. Hill, J. Phys. Chem. B **104**, 6694 (2000).

36 N. A. Spaldin and M. Fiebig, Science **309**, 391 (2005).

37 W. Eerenstein, N.D. Mathur, and J.F. Scott, Nature (London) **44**, 759 (2006).

38 H.J. Xiang, S.-H. Wei, M.-H. Whangbo, and J.L.F. Da Silva, Phys. Rev. Lett. **101**, 037209 (2008).

39 A. Malashevich and D. Vanderbilt, Phys. Rev. Lett. **101**, 037210 (2008).

40 Y. Fang, K. Jin, H. Lu, M. He, C. Wang, J. Wen, and G. Yang, Science China **53**, 852 (2010).

41 R.V.K. Mangalam, N. Ray, U.V. Waghmare, A. Sundaresan, and C.N.R. Rao, Solid State Commun. **149**, 1 (2009).

42 M. Venkatesan, C.B. Fitzgerald, and J.M.D. Coey, Nature **430**, 630 (2004).

43 S. Qin, D. Liu, Z. Zuo, Y. Sang, X. Zhang, F. Zheng, H. Liu, and X.-G. Xu, J. Phys. Chem. Lett. **1**, 238 (2010).

44 D.G. Schlom *et al.*, Mater. Sci. Eng. B **87**, 282 (2001).

45 S.-H. Wei and S. B. Zhang, Phys. Rev. B **66**, 155211 (2002).

46 C. Freysoldt, B. Grabowski, T. Hickel, J. Neugebauer, G. Kresse, A. Janotti, and C.G. Van de Walle, Rev. Mod. Phys. **86**, 253 (2014), and references therein.

47 T. Umeda, J. Isoya, N. Morishita, T. Ohshima, and T. Kamiya, Phys. Rev. B **69**, 121201 (2004).

48 T. Wimbauer, B.K. Meyer, A. Hofstaetter, A. Scharmann, and H. Overhof, Phys. Rev. B **56**, 7384 (1997).

49 T. Shimada, Y. Uratani, and T. Kitamura, Acta Materialia **60**, 6322 (2012), and references therein.

50 Y. Yao and H. Fu, Phys. Rev. B **84**, 064112 (2011).

51 T. Tanaka, K. Matsunaga, Y. Ikuhara, T. Yamamoto, Phys. Rev. B **68**, 205213 (2003).

52 T. Moriya, *Spin fluctuation in itinerant electron magnetism model* (Springer-Verlag, Berlin, 1985).

53 D.I. Khomskii, *Transition metal compounds* (Cambridge University Press, 2014).

54 E.C. Stoner, Proc. R. Soc. London Ser. A **165**, 372 (1938).

55 T. Shimada, Y. Uratani, and T. Kitamura, Appl. Phys. Lett. **100**, 162901 (2012).

56 T. Shimada, T. Ueda, J. Wang, and T. Kitamura, Phys. Rev. B **87**, 174111 (2013).

[57] T. Xu, T. Shimada, Y. Araki, J. Wang, and T. Kitamura, Phys. Rev. B **92**, 104106 (2015).

[58] W. Kohn and L. J. Sham, Phys. Rev. **140**, A1133 (1965).

[59] U. von Barth and L. Hedin, J. Phys. C **5**, 1629 (1972).

[60] P. H. Dederichs, S. Blugel, R. Zeller, and H. Akai, Phys. Rev. Lett. **53**, 2512 (1984).

[61] P. Giannozzi *et al.*, J. Phys. C **21**, 395502 (2009); P. Giannozi *et al.*, http://www.quantum-espresso.org.

[62] N. Troullier and J. L. Martins, Phys. Rev. B **43**, 1993 (1991).

[63] H. Fu and O. Gulseren, Phys. Rev. B **66**, 214114 (2002).

[64] A. Raeliarijaona and H. Fu, Phys. Rev. B **92**, 094303 (2015); J. Appl. Phys. **115**, 054105 (2014).

[65] Z. Alahmed and H. Fu, Phys. Rev. B **76**, 224101 (2007).

[66] R. Wahl, D. Vogtenhuber, and G. Kresse, Phys. Rev. B **78**, 104116 (2008).

[67] J. Harada, T. Pedersen, and Z. Barnea, Acta Cryst. **A26**, 336 (1970).

[68] N. Marzari, D. Vanderbilt, and M. C. Payne Phys. Rev. Lett. **79**, 1337 (1997).

[69] H.J. Monkhorst and J.D. Pack, Phys. Rev. B **13**, 5188 (1976).

[70] J. Heyd, G.E. Scuseria, and M. Ernzerhof, J. Chem. Phys. **118**, 8207 (2003).

[71] D.D. Cuong, B. Lee, K.M. Choi, H.-S. Ahn, S. Han, and J. Lee, Phys. Rev. Lett. **98**, 115503 (2007).

[72] R. Adhikari and H. Fu, J. Appl. Phys. **116**, 123712 (2014).

[73] C. Mitra, C. Lin, J. Robertson, and A.A. Demkov, Phys. Rev. B **86**, 155105 (2012).

[74] N.W. Ashcroft and N.D. Mermin, *Solid State Physics* (Thomson Learning, 1976).

[75] S. Banarjee, A. Datta, A. Bhaumik, and D. Chakravorty, J. Appl. Phys. **110**, 064316 (2011).

TABLE I: Energy difference $\Delta E = E_{\mathrm{GS}} - E_{\mathrm{NM}}$ per supercell (the third column) and the magnitude $|\mathbf{M}|$ of optimal magnetic moment per supercell (the fourth column, in units of μ_B), for different vacancy species and different charge states in $BaTiO_3$.

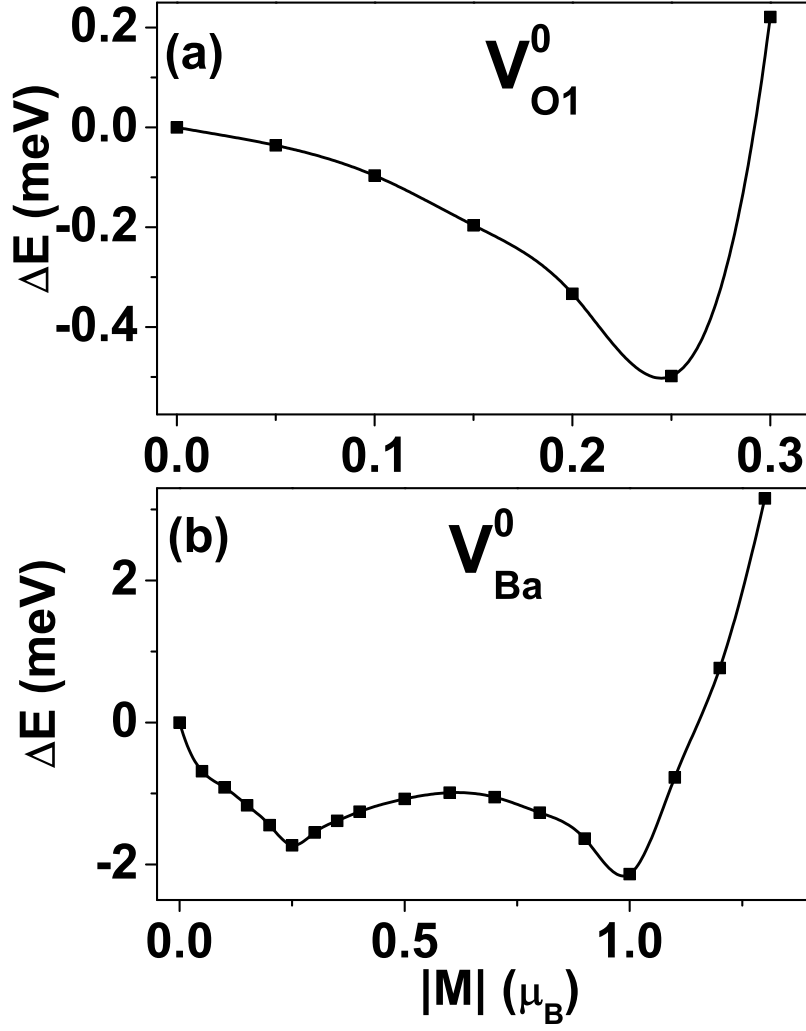| Vacancy	charge q	ΔE (meV)	$|\mathbf{M}|$ (μ_B)
V_{O1}^q	0	-0.5	0.25
	1+	0.0	0.00
	2+	0.0	0.00
V_{O2}^q	0	-0.5	0.25
	1+	0.0	0.00
	2+	0.0	0.00
V_{Ti}^q	0	-20.5	3.50
	1-	-10.4	1.70
	2-	-17.2	1.52
	3-	-6.9	1.00
	4-	0.0	0.00
V_{Ba}^q	0	-2.1	1.00
	1-	0.0	0.00
	2-	0.0	0.00

FIG. 1: The energy difference $\Delta E = E_{\mathrm{GS}} - E_{\mathrm{NM}}$ as a function of the magnitude of magnetic moment, obtained in constrained magnetic-moment calculations, for (a) V_{O1}^0 and (b) V_{Ba}^0.
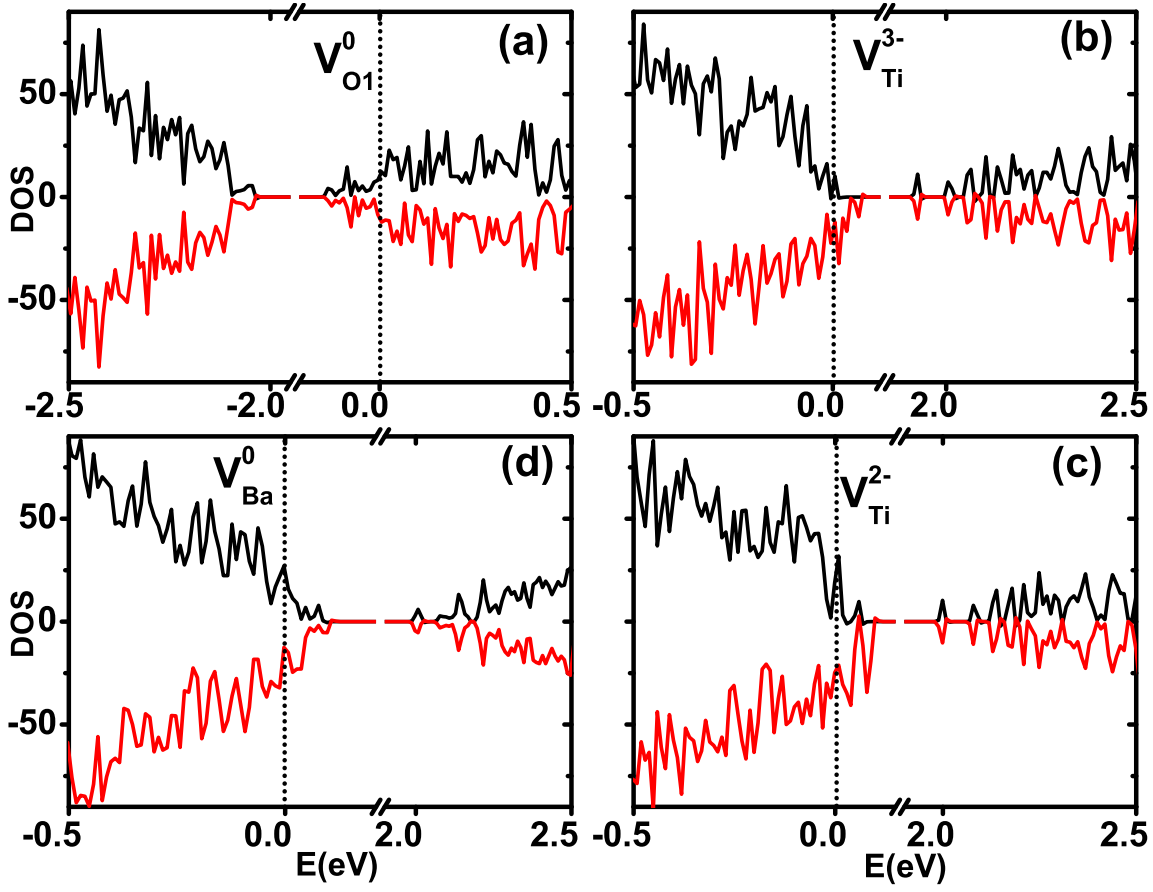
FIG. 2: (Color online) Spin-resolved density of states (DOS) near the Fermi energy E_F for the following vacancies: (a) V_{O1}^0, (b) V_{Ti}^{3-}, (c) V_{Ti}^{2-}, and (d) V_{Ba}^0. Black and red lines are spin-up and spin-down components, respectively; the spin-down component is plotted as negative values. E_F (the dotted line) is chosen to be the zero reference for energy.
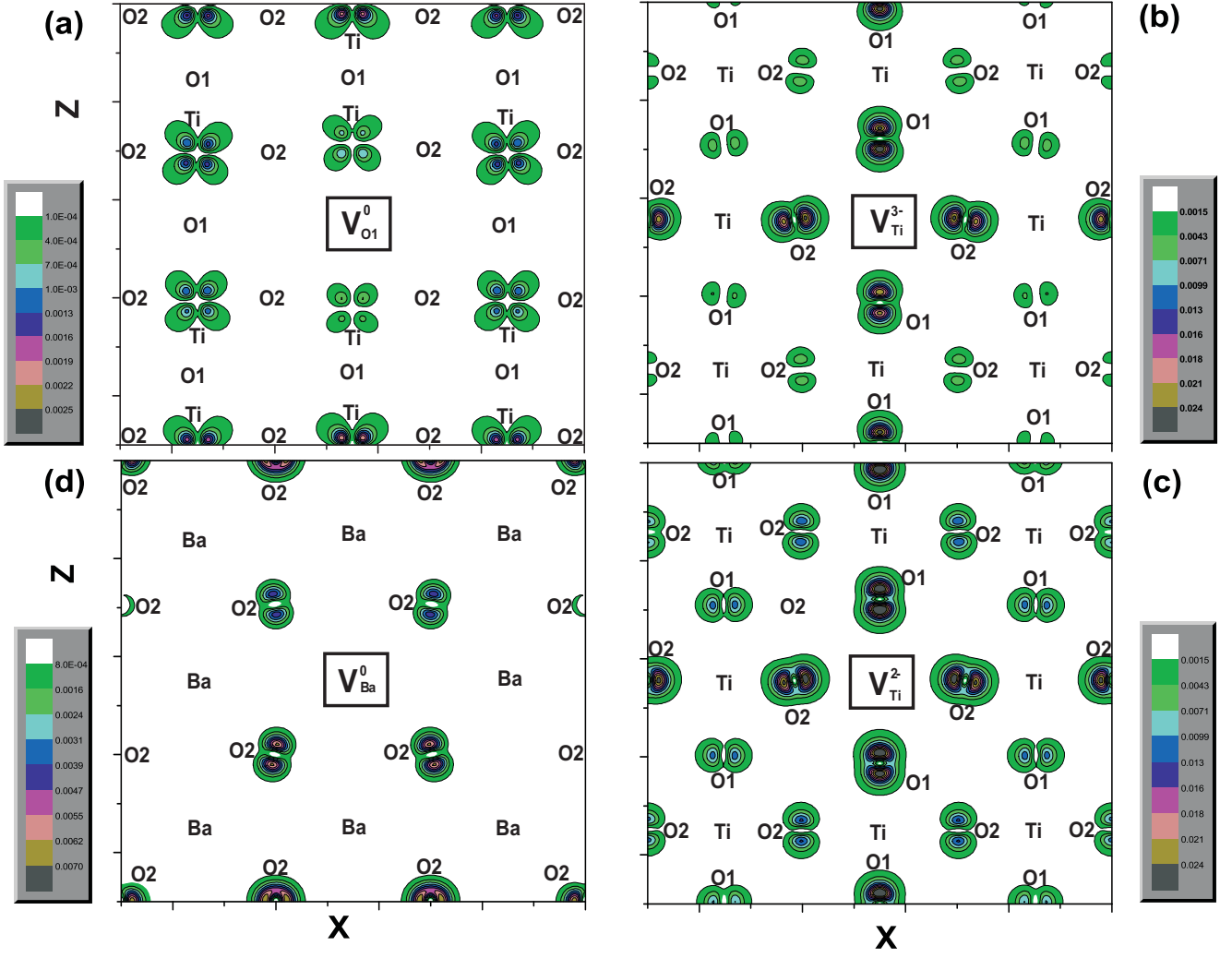
FIG. 3: (Color online) Contour plots of spin density $\Delta\rho(\mathbf{r})$ on a XZ plane that contains the site of vacancy, for the following vacancies: (a) V_{O1}^{0}, (b) V_{Ti}^{3-}, (c) V_{Ti}^{2-}, and (d) V_{Ba}^{0}. To facilitate a better understanding, the locations of atoms on the considered plane are marked by atomic names. The location of the vacancy is marked by a box at the center of each supercell.
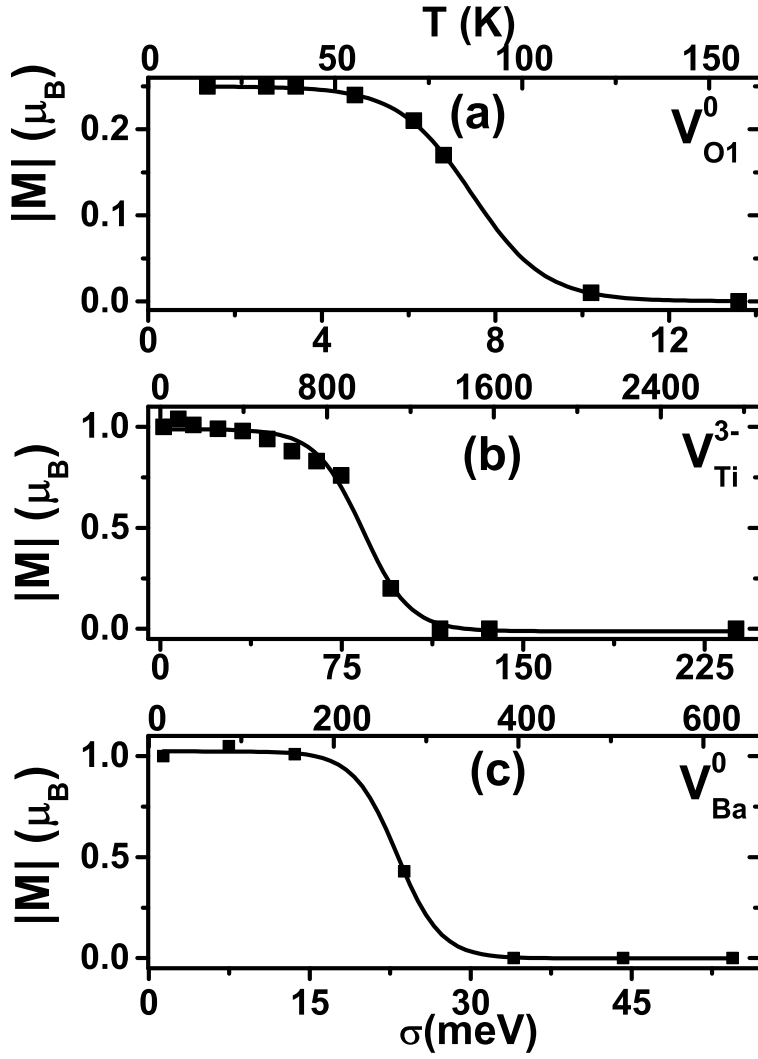
FIG. 4: The DFT-calculated magnetic moment as a function of the temperature-smearing parameter σ for the following vacancies: (a) V_{O1}^0, (b) V_{Ti}^{3-}, and (c) V_{Ba}^0. In each panel, the bottom horizontal axis is σ in units of meV, and the corresponding temperature is given in the top horizontal axis. Symbols are direct calculation results, and solid lines are obtained by analytical fitting.
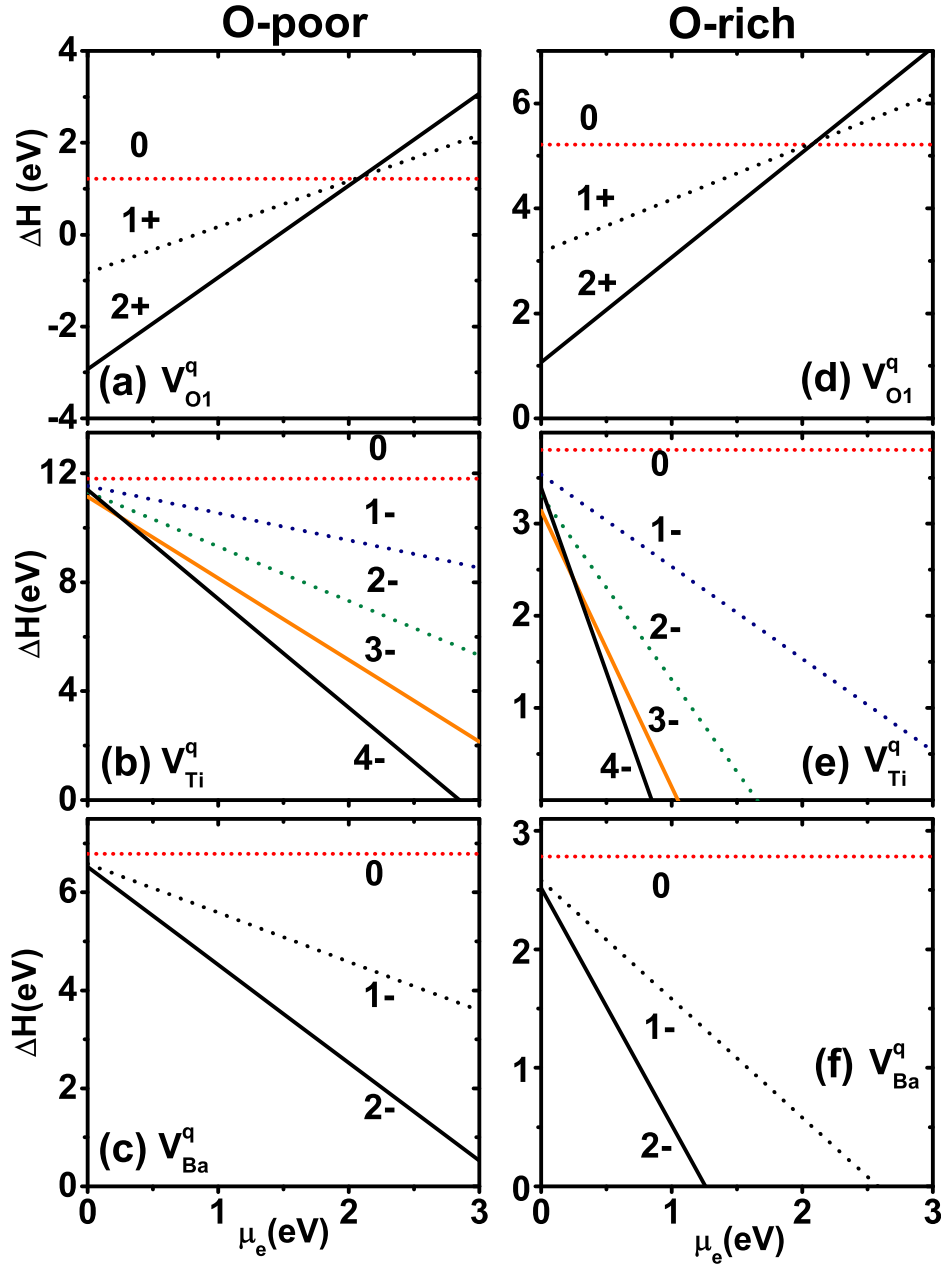
FIG. 5: (Color online) Vacancy formation energies as a function of μ_e for different vacancies. The left column (a)-(c) are for $\mu_O = -4$ eV (which is near the O-poor condition), $\mu_{Ba} = -2.545$ eV, and $\mu_{Ti} = -3.285$ eV. The right column (d)-(e) are for $\mu_O = 0$ eV (which corresponds to the O-rich condition), $\mu_{Ba} = -6.545$ eV, and $\mu_{Ti} = -11.285$ eV.